FRONTIERS OF PHYSICS

RESEARCH ARTICLE
Volume 19 / Issue 4 / 43209 / 2024

A universal non-Hermitian platform for bound state in the continuum enhanced wireless power transfer

Haiyan Zhang[1], Zhiwei Guo[1,†], Yunhui Li[2], Yaping Yang[1], Yuguang Chen[1,‡], Hong Chen[1]

1 School of Physics Science and Engineering, Tongji University, Shanghai 200092, China
2 Department of Electrical Engineering, Tongji University, Shanghai 201804, China
Corresponding authors. E-mail: †2014guozhiwei@tongji.edu.cn, ‡ygchen@tongji.edu.cn
Received December 25, 2023; accepted January 16, 2024

ABSTRACT

Non-Hermitian systems with parity–time (PT)-symmetry have been extensively studied and rapidly developed in resonance wireless power transfer (WPT). The WPT system that satisfies PT-symmetry always has real eigenvalues, which promote efficient energy transfer. However, meeting the condition of PT-symmetry is one of the most puzzling issues. Stable power transfer under different transmission conditions is also a great challenge. Bound state in the continuum (BIC) supporting extreme quality-factor mode provides an opportunity for efficient WPT. Here, we propose theoretically and demonstrate experimentally that BIC widely exists in resonance-coupled systems without PT-symmetry, and it can even realize more stable and efficient power transfer than PT-symmetric systems. Importantly, BIC for efficient WPT is universal and suitable in standard second-order and even high-order WPT systems. Our results not only extend non-Hermitian physics beyond PT-symmetry, but also bridge the gap between BIC and practical application engineering, such as high-performance WPT, wireless sensing and communications.

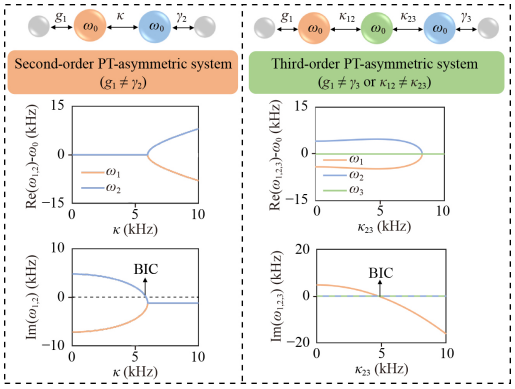

Keywords non-Hermitian physics, parity–time asymmetry, bound state in the continuum, wireless power transfer

1 Introduction

Wireless power transfer (WPT), including radiative transfer [1, 2] and non-radiative near-field transfer [2–18], is a technology of transmitting energy from the source to the load based on electromagnetic waves, breaking the limitations of traditional charging methods with wired cables [19]. Among them, the non-radiative WPT technology based on near-field magnetic resonance has been greatly developed due to its high efficiency and cracking electromagnetic compatibility, and it is also a potential means to power for multiple receivers [11]. Recently, novel physical concepts have emerged, such as anapole [20], topology [21], general parity–time (PT)-symmetry [22], and pseudo-Hermitian physics [23], which have been used to achieve efficient energy transfer. Moreover, concepts derived from non-Hermitian physics and PT-symmetry have attracted considerable attention [24–28]. Importantly, entirely fascinating features related to PT-symmetry ($\widehat{\boldsymbol{H}}PT = PT\widehat{\boldsymbol{H}}$) have sparked intense research into non-Hermitian systems [29]. PT-symmetry originates from quantum mechanics [30, 31] and has been extensively studied in classical wave control, including energy manipulations [5, 9, 13, 32], lasers [33–36], coherent perfect absorber [37, 38], wireless sensing [39–42], etc. Especially, PT-symmetry lays a solid foundation for the design of efficient and robust WPT systems in second-order [3, 43] and even higher-order [9, 13, 15, 44–46] non-

Higher Education Press

https://doi.org/10.1007/s11467-023-1388-x

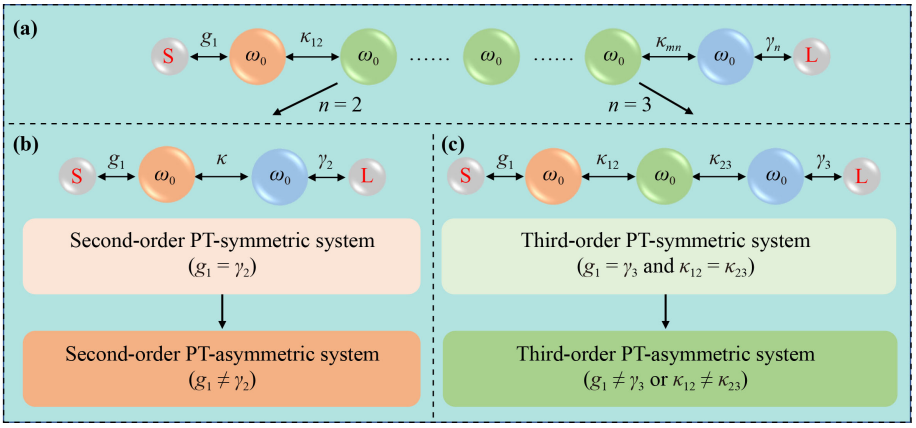

Fig. 1 Schematic diagrams of non-Hermitian models. **(a)** A general non-Hermitian physical model with multiple resonators. **(b)** Second-order non-Hermitian systems, including the PT-symmetric model with balanced gain–loss ($g_1=\gamma_2$), and PT-asymmetric model with unbalanced gain–loss ($g_1\neq\gamma_2$). **(c)** Third-order non-Hermitian systems, including PT-symmetric system with balanced gain–loss ($g_1=\gamma_3$) and symmetric coupling ($\kappa_{12}=\kappa_{23}$), and PT-asymmetric system with unbalanced gain–loss ($g_1\neq\gamma_3$) and/or asymmetric coupling ($\kappa_{12}\neq\kappa_{23}$).

Hermitian systems. For traditional second-order PT-symmetric systems, when the transfer distance changes, it is usually necessary to use frequency tracking technology to achieve high-efficiency WPT in the strong coupling region [3], while in third-order PT-symmetric systems, there is no need to track the operating frequency [9]. However, WPT systems based on PT-symmetry are still limited to harsh operating conditions due to the dependence on the inherently balanced configuration, that is, balanced gain–loss in the second-order system, even simultaneously requiring balanced gain–loss and symmetric coupling in the third-order system, resulting in limited application scenarios. Inspiringly, with the aid of a nonlinear PT-symmetric circuit, the robust WPT can also be realized [5]. However, the WPT system with nonlinear circuit elements usually requires high power input signals, and the working frequency varies with the transfer distance, thus it is not feasible to use a standard source with a fixed working frequency. Therefore, a natural question is whether we can achieve efficient WPT in linear non-Hermitian systems that do not rely on PT-symmetry?

As a kind of electromagnetic mode that is non-radiative yet embedded within the radiation continuum spectrum [47–51], bound state in the continuum (BIC) with high-quality (Q) factor can be used to construct a strong localized field for efficient energy transfer. Generally, BIC can be interpreted as an interference effect in which two or more radiating components cancel each other. Specifically, in the magnetic resonance WPT system composed of resonant coils, BIC modes will promote efficient electromagnetic wave capture to reduce electromagnetic wave leakage into free space, which is benefit to achieving efficient energy transfer [47].

In this work, we propose theoretically and demonstrate experimentally that stable WPT with high efficiency at a fixed working frequency can be realized with the aid of BIC in magnetic resonance-coupled systems. Especially, the purely real steady eigenmode known as BIC supporting maximized transfer efficiency is guaranteed by an optimal gain rate or loss rate, regardless of whether the gain and loss are balanced and the coupling is symmetric or not. Therefore, we can freely choose to adjust the transmitter end or receiver end to realize the BIC mode and high efficiency is maintained across various transfer distances beyond PT-symmetry. It should be emphasized that the BIC-assisted WPT scheme conducted in this work is universal, which is suitable in the standard second-order and even high-order WPT systems. Our results open up new opportunities for the development of near-field control devices with applications in photonics, acoustics and other coupled-wave fields.

2 Results

2.1 Second-order non-Hermitian systems

For a general non-Hermitian system with multiple resonators in Fig. 1(a), the input energy from the left side (source, S) can be transferred to the right side (load, L) based on the mechanism of near-field coupling. Here, we focus on the standard second-order and third-order non-Hermitian systems to demonstrate the BIC-assisted efficient WPT technology. Especially, Fig. 1(b) shows the standard second-order non-Hermitian model, which is composed of a gain resonator with a gain rate g_1 and a loss resonator with a loss rate γ_2. κ denotes the coupling strength between neighboring resonators. When a continuous harmonic wave input with the frequency of ω, $s_{1+}=S_{1+}e^{-i\omega t}$, under the framework of coupled-mode theory, the second-order system dynamics of the system

are represented as [52]

$$\frac{\mathrm{d}a_1}{\mathrm{d}t} = (-\mathrm{i}\omega_0 - g_1 - \Gamma_1)a_1 - \mathrm{i}\kappa a_2 + \sqrt{2g_1}s_{1+}, \tag{1}$$

$$\frac{\mathrm{d}a_2}{\mathrm{d}t} = (-\mathrm{i}\omega_0 - \gamma_2 - \Gamma_2)a_2 - \mathrm{i}\kappa a_1, \tag{2}$$

where $a_m = A_m \mathrm{e}^{-\mathrm{i}\omega t}$ $(m = 1, 2)$ denotes the complex amplitude of the energy stored in each resonant coil. Γ_1 and Γ_2 represent the intrinsic loss of the two resonators, respectively. Such an open system can be equivalent to a closed system when the zero-reflection condition is satisfied [9, 37], that is, $s_{1-} = -s_{1+} + \sqrt{2g_1}a_1 = 0$. A characteristic equation can be obtained to analyze the eigenvalues of the WPT system and the second-order non-Hermitian system with negligible intrinsic loss $(\Gamma_1 = \Gamma_2 = 0)$ is described by

$$\boldsymbol{H}\begin{pmatrix} a_1 \\ a_2 \end{pmatrix} = \omega \begin{pmatrix} a_1 \\ a_2 \end{pmatrix}, \tag{3}$$

and the effective Hamiltonian $\boldsymbol{H}$ can be expressed as

$$\boldsymbol{H} = \begin{pmatrix} \omega_0 + \mathrm{i}g_1 & \kappa \\ \kappa & \omega_0 - \mathrm{i}\gamma_2 \end{pmatrix}. \tag{4}$$

From Eq. (4), it can be clearly seen that for the balanced gain and loss $(g_1 = \gamma_2 = \gamma_0)$, the second-order satisfies PT-symmetry $(PT)\boldsymbol{H}(PT)^{-1} = \boldsymbol{H}$. It is well known that the PT-symmetry provides a convenient way to find the real eigenvalues of non-Hermitian systems, which are useful for efficient WPT. By solving the characteristic equation $|\boldsymbol{H} - \omega\boldsymbol{I}| = 0$ (where $\boldsymbol{I}$ denotes an identity matrix), the eigenvalues of the second-order system can be easily obtained as $\omega_{1,2} = \omega_0 \pm \sqrt{\kappa^2 - \gamma_0{}^2}$. The real eigenvalues of the non-Hermitian system are achieved for the strong coupling condition of $\kappa > \gamma_0$.

In fact, as mentioned in the introductory part, it is urgent for technology to find WPT solutions in PT-asymmetric systems $(g_1 \neq \gamma_2)$. The corresponding eigenvalues are $\omega_{1,2} = \omega_0 + \mathrm{i}\frac{g_1-\gamma_2}{2} \pm \sqrt{\kappa^2 - \left(\frac{g_1+\gamma_2}{2}\right)^2}$. It can be found that when the condition of

$$\kappa^2 = g_1\gamma_2 \tag{5}$$

is satisfied, a stable (real) eigenmode $(\omega_1 = \omega_0)$ called BIC and another unstable (complex) eigenmode $(\omega_2 = \omega_0 + \mathrm{i}g_1 - \mathrm{i}\gamma_2)$ are obtained. It is precisely the BIC with real eigenmode that can be used to implement efficient WPT. Especially, considering a special case of $g_1 = \gamma_2 = \kappa$, which corresponds to the second-order PT-symmetric WPT system. Therefore, the BIC provides a more universal condition for determining the real eigenvalue beyond PT-symmetry.

2.2 Third-order non-Hermitian systems

Similarly, considering a high-order non-Hermitian WPT scheme in Fig. 1(c), which is composed of a gain resonator with a gain rate g_1, a relay resonator, and a loss resonator with the loss rate γ_3. κ_{12} (κ_{23}) denotes the coupling strength between neighboring resonators, and the coupling strength between the nonadjacent resonators is assumed to be negligible. The dynamic evolution equations of the third-order WPT system can be described as follows:

$$\frac{\mathrm{d}a_1}{\mathrm{d}t} = (-\mathrm{i}\omega_0 - g_1 - \Gamma_1)a_1 - \mathrm{i}\kappa_{12}a_2 + \sqrt{2g_1}s_{1+}, \tag{6}$$

$$\frac{\mathrm{d}a_2}{\mathrm{d}t} = (-\mathrm{i}\omega_0 - \Gamma_2)a_2 - \mathrm{i}\kappa_{12}a_1 - \mathrm{i}\kappa_{23}a_3, \tag{7}$$

$$\frac{\mathrm{d}a_3}{\mathrm{d}t} = (-\mathrm{i}\omega_0 - \gamma_3 - \Gamma_3)a_3 - \mathrm{i}\kappa_{23}a_2. \tag{8}$$

Here, the subscripts 1, 2 and 3 refer to the transmitter, relay and receiver coils with the same resonance frequency ω_0. $a_m = A_m \mathrm{e}^{-\mathrm{i}\omega t}$ $(m = 1, 2, 3)$ denotes the complex amplitude of the energy stored in each resonance coil. κ_{12}, κ_{23}, g_1 and γ_3 decay exponentially with the distance between the coils [53].

Using the same analysis method as the second-order WPT system and considering the case with negligible intrinsic loss (i.e., $\Gamma_1 = \Gamma_2 = \Gamma_3 = 0$), a characteristic equation of the third-order non-Hermitian system is described as

$$\boldsymbol{H}\begin{pmatrix} a_1 \\ a_2 \\ a_3 \end{pmatrix} = \omega \begin{pmatrix} a_1 \\ a_2 \\ a_3 \end{pmatrix}, \tag{9}$$

where the effective Hamiltonian is

$$\boldsymbol{H} = \begin{pmatrix} \omega_0 + \mathrm{i}g_1 & \kappa_{12} & 0 \\ \kappa_{12} & \omega_0 & \kappa_{23} \\ 0 & \kappa_{23} & \omega_0 - \mathrm{i}\gamma_3 \end{pmatrix}. \tag{10}$$

By solving the characteristic equation, the eigenfrequencies of the third-order WPT system can be obtained. When the loss and gain are balanced $(g_1 = \gamma_3)$ and the coupling strength is also symmetrical $(\kappa_{12} = \kappa_{23} = \kappa)$, the third-order non-Hermitian system satisfies PT-symmetry, and the real eigenvalues can be guaranteed. However, once the gain and loss are unbalanced $(g_1 \neq \gamma_3)$ or the coupling is asymmetric $(\kappa_{12} \neq \kappa_{23})$, the third-order non-Hermitian system will no longer satisfy PT-symmetry, and there is no clear physical mechanism to find the real eigenvalues of the third-order non-Hermitian system for efficient energy transfer. Surprisingly, the imaginary parts of the eigenfrequencies disappear and the purely real eigenmodes can be obtained when the condition $g_1\left[(\omega - \omega_0)^2 - \kappa_{23}^2\right] = \gamma_3\left[(\omega - \omega_0)^2 - \kappa_{12}^2\right]$ is satisfied. Furthermore, the condition of purely real modes can be summarized into the following two categories:

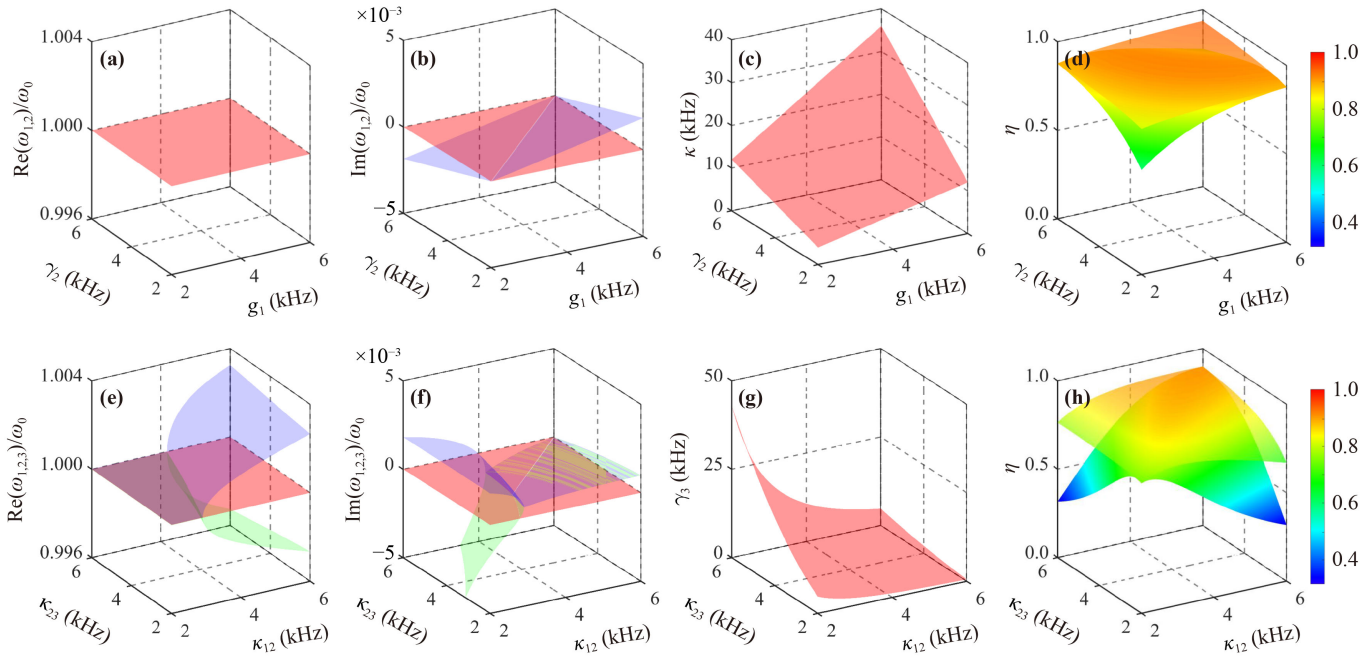

Fig. 2 BIC enabled high-efficient WPT. For the BIC condition of second-order non-Hermitian system $\kappa = \sqrt{g_1\gamma_2}$, the evolution of the real part **(a)** and imaginary part **(b)** of the eigenfrequencies of the system described by Eq. (4) in the two-dimensional parameter space (g_1, γ_2). **(c)** The variation of coupling strength with gain and loss to meet the BIC condition of $\kappa = \sqrt{g_1\gamma_2}$. **(d)** The transfer efficiency of the second-order WPT system with the aid of BIC. (e–h) Same as (a–d), but for the third-order non-Hermitian WPT system. Real **(e)** and imaginary **(f)** parts of the eigenfrequencies of the system described by Eq. (10) in the parameter space of $(\kappa_{12}, \kappa_{23})$ when $g_1 = 4.8$ kHz and $\gamma_3 = g_1\kappa_{23}^2/\kappa_{12}^2$. **(g)** The variation of loss with coupling strengths to meet the BIC condition of $\gamma_3 = g_1\kappa_{23}^2/\kappa_{12}^2$ when $g_1 = 4.8$ kHz. **(h)** The calculated transfer efficiency of the third-order WPT system with the aid of BIC when $g_1 = 4.8$ kHz and $\gamma_3 = g_1\kappa_{23}^2/\kappa_{12}^2$ (upper surface), and balanced gain–loss of $g_1 = \gamma_3 = 4.8$ kHz (lower surface). The intrinsic loss is considered $\Gamma = 0.195$ kHz to match the actual experimental system.

$$g_1(\kappa_{12}^2 - g_1\gamma_3) = \gamma_3(\kappa_{23}^2 - g_1\gamma_3),$$
$$\omega_{2,3} = \omega_. \pm \sqrt{\kappa_{12}^2 + \kappa_{23}^2 - g_1\gamma_3}. \tag{11}$$

$$g_1\kappa_{23}^2 = \gamma_3\kappa_{12}^2, \omega_1 = \omega_0. \tag{12}$$

On the one hand, when the criterion $g_1(\kappa_{12}^2 - g_1\gamma_3) = \gamma_3(\kappa_{23}^2 - g_1\gamma_3)$ in Eq. (11) is satisfied, although the third-order non-Hermitian system has two real eigenfrequencies, they deviate from the resonant frequency of ω_0, resulting in poor stability of the WPT system. On the other hand, according to Eq. (12), a purely real mode (i.e., BIC) at the fixed frequency of $\omega_1 = \omega_0$ can be obtained when the criterion $g_1\kappa_{23}^2 = \gamma_3\kappa_{12}^2$ is satisfied, which means that we can compensate for the impact of asymmetric coupling by adjusting gain or loss in the third-order WPT system without PT-symmetry, leading to flexible application scenarios. Especially, considering a special case of $g_1 = \gamma_3$ and $\kappa_{12} = \kappa_{23}$, which corresponds to the third-order PT-symmetric WPT system. Obviously, for a third-order WPT system with the fixed load denoted by γ_3, one can determine the optimum gain rate of $g_1 = \gamma_3\kappa_{12}^2/\kappa_{23}^2$ to realize BIC for efficient WPT, as implicated by Eq. (12), and vice versa.

2.3 BIC enabled high-efficiency WPT

Then we verify the effectiveness of BIC in achieving efficient WPT in Fig. 2. Considering the BIC condition of the second-order non-Hermitian WPT system given in Eq. (5), the corresponding real and imaginary parts of the eigenfrequencies are shown in Figs. 2(a) and (b), respectively. Especially, under the BIC condition, the coupling strength as the function of g_1 and γ_2 is shown in Fig. 2(c). The power transfer efficiency of the non-Hermitian system $\eta = |s_{2-}/s_{1+}|^2$ can be obtained. Combining the output signal of the receiver $s_{2-} = \sqrt{2\gamma_2}a_2$ with Eqs. (1) and (2), the power transfer efficiency of the non-Hermitian system can be deduced as

$$\eta = \left| \frac{2\sqrt{g_1\gamma_2}\kappa}{\kappa^2 + [\mathrm{i}(\omega - \omega_0) - (g_1 + \Gamma_1)][\mathrm{i}(\omega - \omega_0) - (\gamma_2 + \Gamma_2)]} \right|^2. \tag{13}$$

Therefore, provided that the criterion $\kappa^2 = g_1\gamma_2$ is satisfied, the real mode $\omega = \omega_0$ could exist, which ensures efficient and stable WPT with the efficiency up to 90%, as presented in the upper surface of Fig. 2(d), regardless of whether the gain and loss are balanced or not. Moreover, it needs to be emphasized that BIC not only

provides an alternative solution to replace PT-symmetry to achieve efficient WPT, but also overcomes the efficiency decrease (frequency splitting) limitation of the PT-symmetric scheme in weak (strong) coupling region. By contrast, the transmission performance of the second-order WPT system with the aid of BIC is obviously better than that of the second-order PT-symmetric system shown in the lower surface of Fig. 2(d). More details about the relationship between BIC with the real eigenvalue of the second-order non-Hermitian system and efficient wireless power transfer are given in Supplementary Note 1.

As mentioned above, the key idea of BIC for efficient WPT is universal and can be suitable even for the high-order non-Hermitian WPT system. Considering the BIC of the third-order non-Hermitian system shown in Fig. 1(c), the relationship between the eigenfrequencies and the coupling strengths can also be intuitively presented in a graphical form, as presented in Figs. 2(e) and (f). Here, in order to satisfy the BIC condition $\gamma_3 = g_1\kappa_{23}^2/\kappa_{12}^2$ with a fixed gain rate of $g_1 = 4.8$ kHz, the variation of loss rate with coupling strengths is shown in Fig. 2(g). From Figs. 2(e)–(g), it can be clearly seen that the BIC mode corresponds to a stable real eigenfrequency of ω_0. Similarly, combining the output signal of the receiver end $s_{2-} = \sqrt{2\gamma_3}a_3$ with Eqs. (6)–(8), the transfer efficiency of the third-order non-Hermitian system with actual intrinsic loss ($\Gamma_1 = \Gamma_2 = \Gamma_3 = \Gamma \neq 0$) at $\omega = \omega_0$ can be deduced as

$$\eta = \left| -\frac{2\sqrt{g_1\gamma_3}\kappa_{12}\kappa_{23}}{g_1\kappa_{23}^2+\gamma_3\kappa_{12}^2+(\kappa_{12}^2+\kappa_{23}^2+g_1\gamma_3)\,\Gamma+(g_1+\gamma_3)\,\Gamma^2+\Gamma^3} \right|^2. \tag{14}$$

Compared to the third-order PT-symmetric system with balanced gain–loss (the lower surface), the third-order system with the aid of BIC (the upper surface) can achieve more efficient WPT over a wider range, as shown in Fig. 2(h). The efficiency supported by the BIC mode has a maximum value of around 90% due to the non-negligible intrinsic loss ($\Gamma = 0.195$ kHz) in the actual WPT system. Obviously, the general third-order WPT system has flexible applications, as it is not limited to PT-symmetry conditions. More details about the relationship between BIC with the real eigenvalue of the third-order non-Hermitian system and efficient wireless power transfer are given in Supplementary Note 1.

2.4 Comparison of transmission performance between PT-symmetry and BIC for WPT

To better highlight the advantages of BIC-assisted efficient WPT systems, we compare the transmission performance of the following four WPT models, including second-order (third-order) WPT systems with PT-symmetry and BIC, as shown in Fig. 3. Considering the second-order PT-symmetric WPT system with $g_1 = \gamma_2$, it guarantees the purely real eigenfrequencies in the strong coupling region, as shown by the real and imaginary eigenfrequencies spectrum versus coupling strength κ in Figs. 3(a) and (b), respectively. Especially, the bifurcation associated with the spontaneous symmetry breakdown is marked by the exceptional point (EP). Figure 3(c) gives the transfer efficiency of the PT-symmetric WPT scheme as a function of the coupling strength κ, where the lossless ($\Gamma = 0$ kHz) and lossy ($\Gamma = 0.195$ kHz) systems are shown by the dashed line and solid line, respectively. As explained in the introductory part, PT-symmetry can be used to generate high-efficiency WPT in the strong coupling region, however, complex frequency tracking techniques are required. Importantly, even if the second-order WPT system is not PT-symmetric ($\widehat{\boldsymbol{H}}PT \neq PT\widehat{\boldsymbol{H}}$), that is, $g_1 \neq \gamma_2$, the Hamiltonian can still have a real eigenvalue known as BIC embedded in the weak coupling region, as shown in Figs. 3(d) and (e). Moreover, BIC is locked at the resonance frequency $\omega = \omega_0$, and there is no need to track the working frequency for WPT. From the corresponding transfer efficiency spectrum in Fig. 3(f), it can be clearly seen that compared to traditional second-order PT-symmetric system, second-order PT-asymmetric WPT system with the aid of BIC has more excellent transmission performance.

As for the third-order PT-symmetric WPT system, when the coupling strength changes, there always exists a purely real mode, which enables efficient WPT over a wide range, as presented in Figs. 3(g)–(i). However, the disadvantage is that it requires balanced gain and loss ($g_1 = \gamma_3$), as well as symmetric coupling ($\kappa_{12} = \kappa_{23}$), resulting in harsh operating conditions to meet third-order PT-symmetry. Surprisingly, the efficient WPT mechanism with the aid of BIC can overcome the above two shortcomings. In addition, efficient WPT with good stability can also be achieved in the third-order system beyond PT-symmetry, as shown in Figs. 3(j)–(l). The BIC line used for robust energy transfer is marked in Fig. 3(k). Therefore, the high-performance WPT enabled by BIC at different non-Hermitian systems is theoretically confirmed.

2.5 Experimental demonstration of BIC-assisted efficient WPT

Next, we validate the BIC-assisted efficient energy transfer based on an actual WPT system. The corresponding schematic diagram and experimental diagram of the third-order WPT system are shown in Figs. 4(a) and (b), respectively. More details about the coil fabrication, measurement, and the related second-order WPT system can be found in Supplementary Note 2. In the experiment, signals generated from the port 1 of a vector network analyzer (Keysight E5071C) are transported into a source coil, which works as the source for the

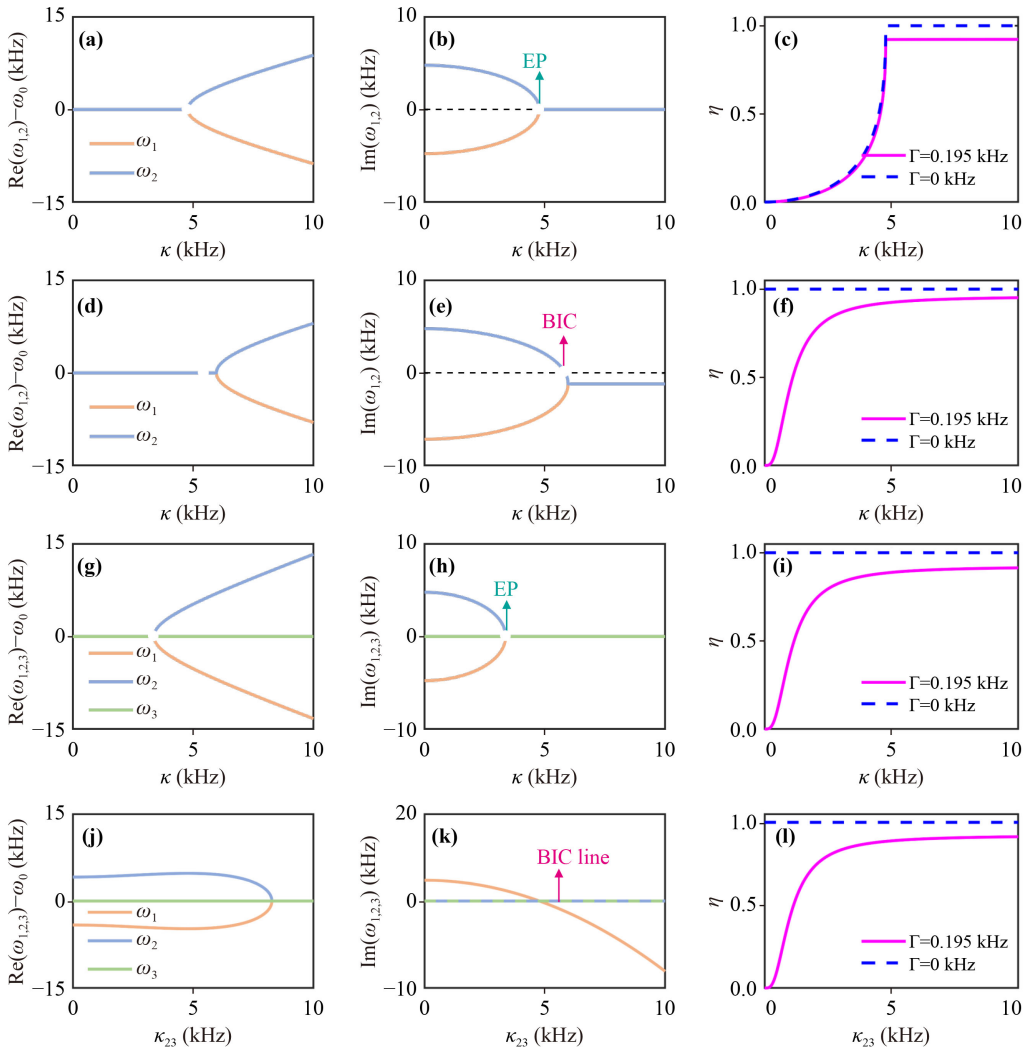

Fig. 3 Comparison of PT-symmetry and BIC for WPT in two different non-Hermitian systems. Evolution of the real part **(a)** and imaginary part **(b)** of the eigenfrequencies in the second-order PT-symmetric system with $g_1 = 4.8$ kHz and $\gamma_2 = 4.8$ kHz. **(c)** The corresponding transfer efficiency versus κ. **(d–f)** Similar to (a–c), but for the BIC-assisted efficient WPT, where the asymmetric parameters are $g_1 = 4.8$ kHz and $\gamma_2 = 7.2$ kHz, respectively. **(g–i)** Same as (a–c), but for the third-order PT-symmetric system with $g_1 = 4.8$ kHz and $\gamma_2 = 4.8$ kHz. **(j–l)** Same as (d–f), but for the BIC-assisted efficient WPT in the third-order non-Hermitian system with $g_1 = 4.8$ kHz and $\gamma_3 = g_1\kappa_{23}^2/\kappa_{12}^2$. The intrinsic loss is considered as $\Gamma = 0.195$ kHz, which is consistent with the actual WPT system composed of lossy coils.

system. The port 2 of the vector network analyzer is connected to the load coil to obtain the output signal through near-field coupling. The impedance of both the source and load is 50 Ω. In addition, the relationships between the coupling strength and the horizontal distance are given in Supplementary Note 3, including $g_1(d_1)$, $\gamma_3(d_2)$, $\kappa_{12}(s_{12})$, $\kappa_{23}(s_{23})$. In fact, the coupling strength between coils is related to many factors, including but not limited to the relative lateral distance of the coils, as well as the relative axial distance and deflection angle [54].

2.6 Flexible regulation of the BIC

The mechanism of BIC-assisted efficient WPT in the third-order non-Hermitian system is widely applicable to varying charging scenarios. Figures 5(a)–(f) present the real and imaginary parts of the eigenfrequencies of the third-order WPT system versus the transfer distance s_{23} at different gain–loss ratios, i.e., $g_1/\gamma_3 = 0.5$, $g_1/\gamma_3 = 1$ and $g_1/\gamma_3 = 2$. κ_{12} is 13.1 kHz because of the fixed $s_{12} =$ 15 cm all the time. From Figs. 5(d)–(f), it is obvious that different gain–loss ratios result in BIC mode appearing at different transfer distances. In other words, by changing the gain–loss ratio, the optimal transfer distance can be flexibly adjusted, which are shown in Figs. 5(g)–(i). Especially, the calculated and measured results are marked by the circles and solid lines, which meet well with each other. The results in Fig. 5 indicate that even in the case of asymmetric coupling ($\kappa_{12} \neq \kappa_{23}$),

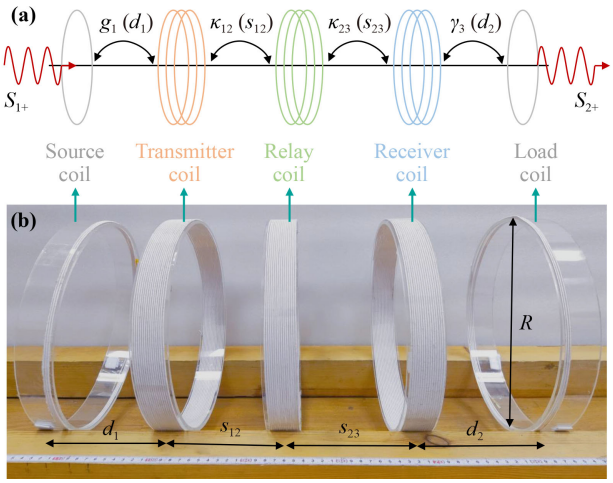

Fig. 4 Third-order non-Hermitian WPT systems. **(a)** Third-order WPT system consisting of three resonant (transmitter, relay and receiver) coils and two non-resonant (source and load) coils. **(b)** The corresponding photograph of the experimental setup.

the system still has a BIC mode with a fixed eigenfrequency of ω_0 for efficient WPT. Moreover, the above discussion is about the case where the gain rate remains unchanged while the loss rate is adjusted to realize BIC mode with efficient WPT. Similarly, the BIC mechanism can also be applied to another case where the loss rate is fixed and the gain rate is adjusted to achieve BIC mode for efficient WPT.

2.7 Advantages of BIC-assisted energy transfer mechanism

Finally, we compare the transmission performance of BIC-assisted systems and the conventional balanced gain–loss systems in Fig. 6. Obviously, whether in second-order WPT systems in Fig. 6(a) or third-order WPT systems in Fig. 6(b), the efficiency of the BIC-assisted WPT systems is higher than that of balanced gain–loss systems. The experimental results (circles) and theoretical calculation results (solid lines) are in good agreement. Furthermore, the efficiency of the third-order system is slightly lower than that of the second-order system because the intrinsic loss of the third-order system is greater. However, compared to the BIC in second-order system satisfying $\kappa^2 = g_1\gamma_2$, the BIC in third-order system has an additional degree of control freedom, as long as the condition $g_1\kappa_{23}^2 = \gamma_3\kappa_{12}^2$ is met. Overall, compared with the standard second-order PT-symmetric system, whose eigenfrequencies are sensitive

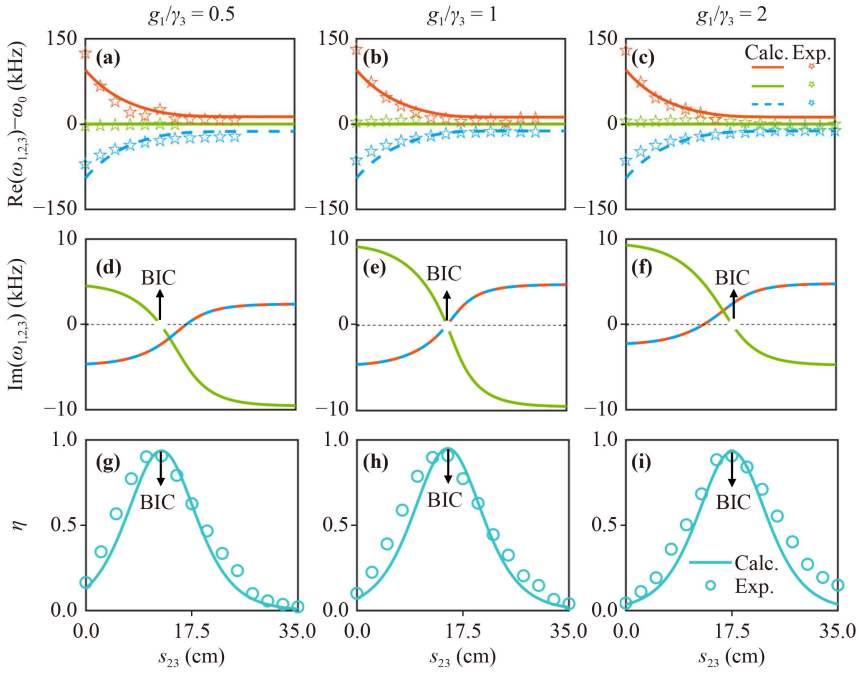

Fig. 5 Flexible regulation of the BIC for efficient WPT in the third-order system. Evolution of the real part and imaginary part of the eigenfrequencies in the third-order non-Hermitian WPT system with different gain–loss ratios: **(a, d)** $g_1/\gamma_3 = 0.5$ ($g_1 = 4.8$ kHz and $\gamma_3 = 9.6$ kHz); **(b, e)** $g_1/\gamma_3 = 1$ ($g_1 = 9.6$ kHz and $\gamma_3 = 9.6$ kHz); **(c, f)** $g_1/\gamma_3 = 2$ ($g_1 = 9.6$ kHz and $\gamma_3 = 4.8$ kHz). The coupling strength between the transmitter coil and relay coil is fixed, that is, $\kappa_{12} = 13.1$ kHz with $s_{12} = 15$ cm. The solid line and the pentagram represent the theoretical and experimental results respectively. **(g–i)** Similar to (a–f), but for the power transfer efficiency versus s_{23} at the fixed working frequency ω_0. The BIC with real eigenvalue $\omega_1 = \omega_0$ is marked by the black arrow. The intrinsic loss of the resonant coil is $\Gamma = 0.195$ kHz. The calculated (measured) transfer efficiency is marked by solid lines (circles).

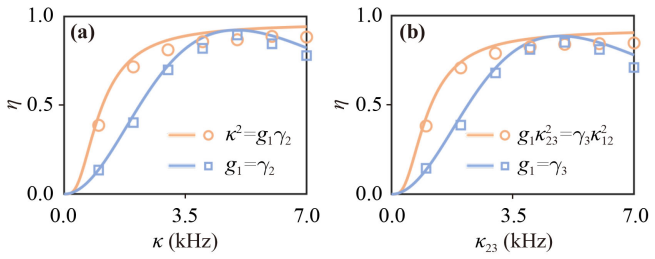

Fig. 6 Comparison of transfer efficiency between BIC-assisted systems and balanced gain–loss systems. **(a)** The transfer efficiency of second-order WPT systems: balanced gain–loss system ($g_1 = \gamma_2 = 4.8$ kHz), and BIC-assisted system ($g_1 = 4.8$ kHz and $\gamma_2 = \kappa^2/g_1$). **(b)** Same as (a), but for the third-order WPT systems: balanced gain–loss system ($g_1 = \gamma_3 = 4.8$ kHz), and BIC-assisted system ($g_1 = 4.8$ kHz and $\gamma_3 = g_1\kappa_{23}^2/\kappa_{12}^2$). The calculated and experimental results are marked by solid lines and circles respectively.

to the change of coupling strength in the strong coupling region, the proposed second-order WPT system with the aid of BIC is more stable and robust, since there is always a purely real mode locked at the resonance frequency of ω_0, which is independent of the coupling strength. Moreover, the BIC-assisted third-order WPT system relaxes the limitation of balanced gain–loss and symmetric coupling, which are required in the conventional third-order PT-symmetric system. In addition, the degree of freedom to adjust and realize the real mode known as BIC includes the gain rate at the transmitter end and the loss rate at the receiver end at a fixed transfer distance. Surprisingly, by tuning appropriate non-Hermitian parameters, such as gain rate or loss rate, BIC mode always exists in third-order WPT systems. Therefore, the presented BIC scheme is of benefit to apply to flexible wireless charging scenarios. Also, the WPT mechanism with the aid of BIC can be generalized to apply in multi-load charging scenarios, and the detailed discussion on the application of multi-load charging is given in Supplementary Note 4. Furthermore, the proposed WPT mechanism may be extended to achieve the purely real mode with stable frequency in anti-PT symmetric systems, where the coupling strengths are pure imaginary [39].

3 Conclusion

In summary, we propose a general non-Hermitian WPT system for efficient and stable WPT at a fixed working frequency with the aid of BIC, which is explained by the interference effect of two or more radiation components canceling each other, where the resonant coils can capture electromagnetic waves between them to reduce electromagnetic wave leakage into free space. Importantly, the novel WPT mechanism with improved efficiency, stability and flexibility has been verified theoretically and experimentally in both second-order and third-order WPT systems. It can be expected that the WPT mechanism with the aid of BIC can provide efficient power transfer for a variety of consumer electronics, electric vehicles, and medical devices. In addition, our research has bridged the gap between PT-asymmetric systems and practical application engineering, and may open a door for promoting non-Hermitian physics with PT-asymmetry in other fields such as wireless communication and wireless sensing.

Declarations The authors declare that they have no competing interests and there are no conflicts.

Data and code availability All the data and codes that support the findings of this study are available from the corresponding authors upon reasonable request.

Author contributions Z. G., Y. C., and H. C. conceived the idea and supervised the project. H. Z. carried out the analytical calculations with the help of Y. Y., H. Z. prepared the sample and conducted experimental measurements with the help of Y. L., H. Z., Z. G., Y.C., and H. C. wrote the manuscript. All authors contributed to discussions of the results and the manuscript.

Electronic supplementary materials Supplementary materials to this article can be found online at https://doi.org/10.1007/s11467-023-1388-x and https://journal.hep.com.cn/fop/EN/10.1007/s11467-023-1388-x.

Acknowledgements This work was supported by the National Key R&D Program of China (Nos. 2021YFA1400602 and 2023YFA1407600), the National Natural Science Foundation of China (Nos. 12004284 and 12374294), the Fundamental Research Funds for the Central Universities (No. 22120210579), and the Chenguang Program of Shanghai (No. 21CGA22).

References

1. A. Krasnok, D. G. Baranov, A. Generalov, S. Li, and A. Alu, Coherently enhanced wireless power transfer, *Phys. Rev. Lett.* 120(14), 143901 (2018)
2. M. Song, P. Jayathurathnage, E. Zanganeh, M. Krasikova, P. Smirnov, P. Belov, P. Kapitanova, C. Simovski, S. Tretyakov, and A. Krasnok, Wireless power transfer based on novel physical concepts, *Nat. Electron.* 4(10), 707 (2021)
3. A. Kurs, A. Karalis, R. Moffatt, J. D. Joannopoulos, P. Fisher, and M. Soljačić, Wireless power transfer via strongly coupled magnetic resonances, *Science* 317(5834), 83 (2007)
4. Y. Xie, Z. Zhang, Y. Lin, T. Feng, and Y. Xu, Magnetic quasi-bound state in the continuum for wireless power transfer, *Phys. Rev. Appl.* 15(4), 044024 (2021)
5. S. Assawaworrarit, X. Yu, and S. Fan, Robust wireless power transfer using a nonlinear parity–time-symmetric circuit, *Nature* 546(7658), 387 (2017)

6. J. Li and B. Zhang, A wireless power transfer system based on quasi-parity–time symmetry with gain–loss ratio modulation, *Int. J. Circuit Theory Appl.* 51(3), 1039 (2023)
7. Z. Miao, D. Liu, and C. Gong, Efficiency enhancement for an inductive wireless power transfer system by optimizing the impedance matching networks, *IEEE Trans. Biomed. Circuits Syst.* 11(5), 1160 (2017)
8. J. Song, F. Yang, Z. Guo, X. Wu, K. Zhu, J. Jiang, Y. Sun, Y. Li, H. Jiang, and H. Chen, Wireless power transfer via topological modes in dimer chains, *Phys. Rev. Appl.* 15(1), 014009 (2021)
9. Z. Guo, J. Jiang, X. Wu, H. Zhang, S. Hu, Y. Wang, Y. Li, Y. Yang, and H. Chen, Rotation manipulation of high-order PT-symmetry for robust wireless power transfer, *Fundamental Res.*, doi: 10.1016/j.fmre.2023.11.010 (2023)
10. Z. Guo, F. Yang, H. Zhang, X. Wu, Q. Wu, K. Zhu, J. Jiang, H. Jiang, Y. Yang, Y. Li, and H. Chen, Level pinning of anti-PT symmetric circuits for efficient wireless power transfer, *Natl. Sci. Rev.* 11(1), nwad172 (2023)
11. B. L. Cannon, J. F. Hoburg, D. D. Stancil, and S. C. Goldstein, Magnetic resonant coupling as a potential means for wireless power transfer to multiple small receivers, *IEEE Trans. Power Electron.* 24(7), 1819 (2009)
12. L. Zhang, Y. Yang, Z. Jiang, Q. Chen, Q. Yan, Z. Wu, B. Zhang, J. Huangfu, and H. Chen, Demonstration of topological wireless power transfer, *Sci. Bull. (Beijing)* 66(10), 974 (2021)
13. M. Sakhdari, M. Hajizadegan, and P. Y. Chen, Robust extended-range wireless power transfer using a higher-order PT-symmetric platform, *Phys. Rev. Res.* 2(1), 013152 (2020)
14. J. Zhou, B. Zhang, W. Xiao, D. Qiu, and Y. Chen, Nonlinear parity–time-symmetric model for constant efficiency wireless power transfer: Application to a drone-in-flight wireless charging platform, *IEEE Trans. Ind. Electron.* 66(5), 4097 (2019)
15. H. Kim, S. Yoo, H. Joo, J. Lee, D. An, S. Nam, H. Han, D. H. Kim, and S. Kim, Wide-range robust wireless power transfer using heterogeneously coupled and flippable neutrals in parity–time symmetry, *Sci. Adv.* 8(24), eabo4610 (2022)
16. Z. Guo, Y. Long, H. Jiang, J. Ren, and H. Chen, Anomalous unidirectional excitation of high-k hyperbolic modes using all-electric metasources, *Adv. Photonics* 3(3), 036001 (2021)
17. A. P. Sample, D. A. Meyer, and J. R. Smith, Analysis, experimental results, and range adaptation of magnetically coupled resonators for wireless power transfer, *IEEE Trans. Ind. Electron.* 58(2), 544 (2011)
18. C. Zeng, Z. Guo, K. Zhu, C. Fan, G. Li, J. Jiang, Y. Li, H. Jiang, Y. Yang, Y. Sun, and H. Chen, Efficient and stable wireless power transfer based on the non-Hermitian physics, *Chin. Phys. B* 31(1), 010307 (2022)
19. N. Tesla, Apparatus for transmitting electrical energy, *U. S. Patent* 1, 119,732 (1914)
20. T. Huang, B. Wang, W. Zhang, and C. Zhao, Ultracompact energy transfer in anapole-based metachains, *Nano Lett.* 21(14), 6102 (2021)
21. B. X. Wang and C. Y. Zhao, Topological phonon polariton enhanced radiative heat transfer in bichromatic nanoparticle arrays mimicking Aubry–André–Harper model, *Phys. Rev. B* 107(12), 125409 (2023)
22. Y. Wu, L. Kang, and D. H. Werner, Symmetry in non-Hermitian wireless power transfer systems, *Phys. Rev. Lett.* 129(20), 200201 (2022)
23. X. Hao, K. Yin, J. Zou, R. Wang, Y. Huang, X. Ma, and T. Dong, Frequency-stable robust wireless power transfer based on high-order pseudo-Hermitian physics, *Phys. Rev. Lett.* 130(7), 077202 (2023)
24. A. Li, H. Wei, M. Cotrufo, W. Chen, S. Mann, X. Ni, B. Xu, J. Chen, J. Wang, S. Fan, C. W. Qiu, A. Alù, and L. Chen, Exceptional points and non-Hermitian photonics at the nanoscale, *Nat. Nanotechnol.* 18(7), 706 (2023)
25. C. Liang, Y. Tang, A. N. Xu, and Y. C. Liu, Observation of exceptional points in thermal atomic ensembles, *Phys. Rev. Lett.* 130(26), 263601 (2023)
26. Y. Li, Y. Ao, X. Hu, C. Lu, C. T. Chan, and Q. Gong, Unsupervised learning of non-Hermitian photonic bulk topology, *Laser Photonics Rev.* 17(12), 2300481 (2023)
27. S. Ke, W. Wen, D. Zhao, and Y. Wang, Floquet engineering of the non-Hermitian skin effect in photonic waveguide arrays, *Phys. Rev. A* 107(5), 053508 (2023)
28. S. M. Zhang and L. Jin, Localization in non-Hermitian asymmetric rhombic lattice, *Phys. Rev. Res.* 2(3), 033127 (2020)
29. R. El-Ganainy, K. G. Makris, M. Khajavikhan, Z. H. Musslimani, S. Rotter, and D. N. Christodoulides, Non-Hermitian physics and PT symmetry, *Nat. Phys.* 14(1), 11 (2018)
30. C. M. Bender, S. Boettcher, and P. N. Meisinger, PT-symmetric quantum mechanics, *J. Math. Phys.* 40(5), 2201 (1999)
31. C. M. Bender and S. Boettcher, Real spectra in non-Hermitian Hamiltonians having PT symmetry, *Phys. Rev. Lett.* 80(24), 5243 (1998)
32. J. Schindler, A. Li, M. C. Zheng, F. M. Ellis, and T. Kottos, Experimental study of active LRC circuits with PT symmetries, *Phys. Rev. A* 84(4), 040101 (2011)
33. S. Longhi, PT-symmetric laser absorber, *Phys. Rev. A* 82(3), 031801 (2010)
34. Y. D. Chong, L. Ge, and A. D. Stone, PT-symmetry breaking and laser-absorber modes in optical scattering systems, *Phys. Rev. Lett.* 106(9), 093902 (2011)
35. Z. Gao, S. T. M. Fryslie, B. J. Thompson, P. S. Carney, and K. D. Choquette, Parity–time symmetry in coherently coupled vertical cavity laser arrays, *Optica* 4(3), 323 (2017)
36. J. M. Lee, S. Factor, Z. Lin, I. Vitebskiy, F. M. Ellis, and T. Kottos, Reconfigurable directional lasing modes in cavities with generalized PT symmetry, *Phys. Rev. Lett.* 112(25), 253902 (2014)
37. Y. Sun, W. Tan, H. Q. Li, J. Li, and H. Chen, Experimental demonstration of a coherent perfect absorber with PT phase transition, *Phys. Rev. Lett.* 112(14), 143903 (2014)
38. C. Wang, W. R. Sweeney, A. D. Stone, and L. Yang, Coherent perfect absorption at an exceptional point, *Science* 373(6560), 1261 (2021)
39. M. Hajizadegan, M. Sakhdari, S. Liao, and P. Y. Chen,

High-sensitivity wireless displacement sensing enabled by PT-symmetric telemetry, *IEEE Trans. Antenn. Propag.* 67(5), 3445 (2019)
40. M. Sakhdari, M. Hajizadegan, Q. Zhong, D. N. Christodoulides, R. El-Ganainy, and P. Y. Chen, Experimental observation of PT symmetry breaking near divergent exceptional points, *Phys. Rev. Lett.* 123(19), 193901 (2019)
41. Z. Xiao, H. Li, T. Kottos, and A. Alu, Enhanced sensing and nondegraded thermal noise performance based on PT-symmetric electronic circuits with a sixth-order exceptional point, *Phys. Rev. Lett.* 123(21), 213901 (2019)
42. Z. Guo, T. Zhang, J. Song, H. Jiang, and H. Chen, Sensitivity of topological edge states in a non-Hermitian dimer chain, *Photon. Res.* 9(4), 574 (2021)
43. Y. Qu, B. Zhang, W. Gu, J. Li, and X. Shu, Distance extension of S-PS wireless power transfer system based on parity–time symmetry, *IEEE Trans. Circuits Syst. II Express Briefs* 70(8), 2954 (2023)
44. J. Kim, H.-C. Son, K.-H. Kim, and Y.-J. Park, Efficiency analysis of magnetic resonance wireless power transfer with intermediate resonant coil, *IEEE Antennas Wirel. Propag. Lett.* 10, 389 (2011)
45. C. Saha, I. Anya, C. Alexandru, and R. Jinks, Wireless power transfer using relay resonators, *Appl. Phys. Lett.* 112(26), 263902 (2018)
46. H. Chen, D. Qiu, C. Rong, and B. Zhang, A double-transmitting coil wireless power transfer system based on parity time symmetry principle, *IEEE Trans. Power Electron.* 38(11), 13396 (2023)
47. C. W. Hsu, B. Zhen, A. D. Stone, J. D. Joannopoulos, and M. Soljačić, Bound states in the continuum, *Nat. Rev. Mater.* 1(9), 16048 (2016)
48. J. Wang, L. Shi, and J. Zi, Spin Hall effect of light via momentum-space topological vortices around bound sates in the continuum, *Phys. Rev. Lett.* 129(23), 236101 (2022)
49. H. Zhang, S. Liu, Z. Guo, S. Hu, Y. Chen, Y. Li, Y. Li, and H. Chen, Topological bound state in the continuum induced unidirectional acoustic perfect absorption, *Sci. China Phys. Mech. Astron.* 66(8), 284311 (2023)
50. X. X. Wang, Z. Guo, J. Song, H. Jiang, H. Chen, and X. Hu, Unique Huygens–Fresnel electromagnetic transportation of chiral Dirac wavelet in topological photonic crystal, *Nat. Commun.* 14(1), 3040 (2023)
51. Q. Wang, C. Zhu, X. Zheng, H. Xue, B. Zhang, and Y. D. Chong, Continuum of bound states in a non-Hermitian model, *Phys. Rev. Lett.* 130(10), 103602 (2023)
52. S. Fan, W. Suh, and J. D. Joannopoulos, Temporal coupled-mode theory for the Fano resonance in optical resonators, *J. Opt. Soc. Am. A* 20(3), 569 (2003)
53. Z. Guo, H. Jiang, Y. Li, H. Chen, and G. S. Agarwal, Enhancement of electromagnetically induced transparency in metamaterials using long range coupling mediated by a hyperbolic material, *Opt. Express* 26(2), 627 (2018)
54. H. Zhang, K. Zhu, Z. Guo, Y. Chen, Y. Sun, J. Jiang, Y. Li, Z. Yu, and H. Chen, Robustness of wireless power transfer systems with parity–time symmetry and asymmetry, *Energies* 16(12), 4605 (2023)